BULLETIN OF THE POLISH ACADEMY OF SCIENCES
TECHNICAL SCIENCES, Vol. 69(6), 2021, Article number: e139205
DOI: 10.24425/bpasts.2021.139205

Experimental studies and modeling of four-wheeled mobile robot motion taking into account wheel slippage

Anna JASKOT[1*] and Bogdan POSIADAŁA[2]

[1] Czestochowa University of Technology, Faculty of Civil Engineering, ul. Akademicka 3, 42-201 Częstochowa, Poland
[2] Czestochowa University of Technology, Faculty of Mechanical Engineering and Computer Science, ul. Dąbrowskiego 73, 42-201 Częstochowa, Poland

Abstract. In the article the results of simulation and experimental studies of the movement of a four-wheeled mobile platform, taking into account wheel slip have been presented. The simulation results have been based on the dynamics of the four-wheel mobile platform. The dynamic model of the system motion takes into account the relationship between the active and passive forces accompanying the platform motion, especially during wheel slip. The formulated initial problem describing the motion of the system has been solved by the Runge-Kutta method of the fourth order. The proposed computational model including the platform dynamics model has been verified in experimental studies using the LEO Rover robot. The motion parameters obtained on the basis of the adopted computational model in the form of trajectories, velocities and accelerations have been compared with the results of experimental tests, and the results of this comparison have been included in the paper. The proposed computational model can be useful in various situations, e.g., real-time control, where models with a high degree of complexity are useless due to the computation time. The simulation results obtained on the basis of the proposed model are sufficiently compatible with the results of experimental tests of motion parameters obtained for the selected type of mobile robot.

Key words: motion dynamics; wheel slippage; wheeled mobile platforms; equations of motion.

1. INTRODUCTION

The aim of the work on modelling the dynamics of motion is primarily to develop computational models supporting the processes of designing and building working machines, including mobile robots, in order to improve their efficiency and reliability. Many models describing the motion of vehicles and mobile robots using the description of the dynamics of objects of varying complexity can be found in literature, which has been described, among others, in the works [1, 2]. In certain situations, e.g., real-time control, models with a high degree of complexity are useless due to the computation time. Therefore, simplified models are sought that can sufficiently reflect the properties of real objects and be useful in such situations. The description of the platform motion proposed in the work is a proposal of such a model. Mobile platforms are used in many aspects of life. Initial research on the phenomena described in the paper concerned kinematics. It was also described in [3]. However, the equations of dynamics have not been considered in this work. The authors of [4] have described a dynamic model with consideration of a floating base with unstable wheel-ground contacts. In the work [5] a control solution for the waypoint tracking problem for a vehicle with a differential drive has been presented. Kinematic control justified for motion control in a limited speed range, when the reference motion is properly designed, has also been proposed. The design of a three-wheeled mobile robot mechanism with a description of the kinematics model and motion control with a collision-free human tracking algorithm have been described in [6]. The tracking control problem and solutions for the three wheeled robot have been proposed in [7], as well for the two wheeled mobile robots in formations in [8]. When designing wheeled mobile robots, it is difficult to properly describe and solve the problems of kinematics and dynamics of motion. In the case of omni-directional robots, they result from nonholonomic system uncertainties and possible external disturbances. Solutions to such problems have been proposed by the authors of the work [9]. Based on the differential equations of motion, the motion parameters can be determined using numerical integration methods, as described, for example, in [9, 10] or in [11], where the Runge-Kutta method of the fourth order has been used. In the description of the motion of mobile platforms, kinematic models of the motion of such objects have been often used in the control process. However, in slip conditions, they lose their application because the conditions of kinematic constraints resulting from the design features of the described object have not met. Therefore, there is a need to search for computational models based on the description of the dynamics of the object's motion with a description of additional phenomena, including the description of the relationship of active and passive forces in the contact zones of the platform wheels with the ground under slip conditions. In this

*e-mail: anna.jaskot@pcz.pl

Manuscript submitted 2021-04-30, revised 2021-07-06, initially accepted for publication 2021-08-09, published in December 2021

paper a computational model built in order to simulate the platform motion has been proposed with the use of a simplified model of platform dynamics and a computational algorithm enabling the tracking of active and passive force relations during wheel slip during the simulation of motion. On the basis of the proposed computational model, it is possible to determine the platform movement parameters, also in the conditions of wheel slip. Models of dynamics of motion, as well as examples of motion simulations made on their basis, have been described in the works [12–14]. The platform motion models presented in these works have been supplemented in this paper with the results of experimental studies, which allowed to verify the correctness of the description of the mobile platform movement parameters on the basis of the applied dynamic models. Experimental and simulation tests have been carried out in relation to the LEO Rover four-wheeled mobile robot, for which a computational model has been developed based on the methodology described in the above-mentioned works. The Runge-Kutta method of the fourth order has been used to integrate the equations of motion. The research on the skid of wheeled mobile robots has been initially carried out by assuming pure rolling of the wheel, which consequently indicated that the longitudinal or lateral skid in the contact of the wheel with the ground does not occur, i.e., it is equal to zero [15, 16]. Indeed, this has little effect if the subject moves over a smooth, flat surface at low velocity values. In this study, the possibility of a slip occurrence has been demonstrated even at low speeds of the mobile robot's motion. On the basis of the motion dynamics model presented in the work, simulations of motion have been carried out in order to obtain the system response to the given forcings. The proposed model of motion dynamics has been verified by examining the real motion of the robot. The obtained motion parameters in the form of displacements, velocities and accelerations have been compared with the results of experimental tests, and the results of this comparison have been included in the paper. The experimental and simulation tests heve been carried out on the LEO Rover robot. The sufficient compatiblity has been demonstrated of the simulation results obtained on the basis of the adopted model with the results of experimental tests of motion parameters obtained for the selected type of mobile robot.

2. MODEL OF DYNAMICS OF MOTION OF A FOUR-WHEEL MOBILE PLATFORM

The dynamics of motion model has been built on the basis of the four-wheeled mobile platform design and has been shown in Fig. 1. The platform's motion model has been built on the basis of the description of the rigid body motion and the motion is realized on a flat surface. The motion of the platform has been described in the *OXYZ* reference frame with the beginning at point *O*. The movable Cxyz coordinate system associated with the platform with the beginning at point C, which is the center of mass of the object, has also been adopted for the description. The relative motion of the system elements described in the space of the $O_i x_i y_i z_i$ (movable systems related to the wheels of the platform) in the Cxyz system is translational motion, which results from adopting the directions of the respective axis directions as parallel. Plane motion is a combination of the translational motion of the center of mass and the rotational motion around the center of mass. The coordinates of the position of the center of mass C have been defined by the vector $\mathbf{r}(t)$ with coordinates $X(t)$ and $Y(t)$ as well as the plane rotation angle $\beta(t)$. In order to determine absolute motion in a fixed frame of reference, one should define the relative motion of all O_i modules in the Cxyz moving system, and then describe the motion of the moving system in inertial system OXYZ. The $\mathbf{e}_1$, $\mathbf{e}_2$, $\mathbf{e}_3$ are related to the OXYZ stationary system, while **i**, **j**, **k** are related to the Cxyz and $O_i x_i y_i z_i$ movable systems.

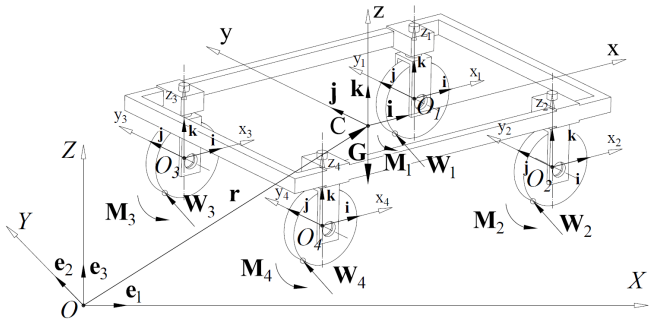

Fig. 1. Model of a four-wheeled mobile platform

Considering the motion of the system as a rigid body, attention should be paid to the motion of individual wheels of the platform. The dynamics research focuses on the analysis of active and passive forces applied to the platform wheels during movement, also with their different orientation in relation to the platform frame. The parameters of the wheel motion result from the set course of the drive torque values and the conditions of the contact wheel with the ground. In the research it has been assumed that the mass of the platform does not change during the motion. The equation of the progressive motion of the four-wheeled mobile platform can be written in the form:

$$m\mathbf{a} = \sum_{i=1}^{5} \mathbf{W}_i \,, \tag{1}$$

where: m – total mass of the mobile platform, $\mathbf{a}$ – acceleration vector of the platform's center of mass, $\mathbf{W}_i$ (for $i = 1,2,3,4$) – the resultant vector of forces occurring at the i-th wheel and $\mathbf{W}_5 = \mathbf{G}$, $\mathbf{G}$ – weight of the platform.

Under the influence of the set active forces and the passive forces occurring during the movement, the parameters of the movement have been determined. The rotation of the rigid body representing the platform has been described as rotation around the point where the center of mass of the system is located. The equation of motion around the center of mass results from the principle that the derivative of the torsion with respect to time is equal to the geometric sum of the moments of the forces external to the center of mass, according to the formula:

$$\frac{\mathrm{d}\mathbf{K}}{\mathrm{d}t} = \sum_{i=1}^{5} \mathbf{s}_i \times \mathbf{W}_i + \sum_{i=1}^{4} \mathbf{M}_i \,, \tag{2}$$

where: $\mathbf{K}$ – angular momentum vector, $\mathbf{s}_i$ – position vectors of resultant forces, $\mathbf{M}_i$ – moment from external forces.

The position vector $\mathbf{r}$ defines the position of the point C in the stationary system, where the center of mass of the system lies and where the origin of the moving system was. The resultant forces have been determined according to the formula:

$$\mathbf{W}_i = \mathbf{F}_{ci} + \mathbf{F}_{oi} + \mathbf{T}_{wi} + \mathbf{T}_{pi} + \mathbf{N}_i, \tag{3}$$

where: $\mathbf{F}_{ci}$ – active forces, $\mathbf{F}_{oi}$ – motion resistance forces, $\mathbf{T}_{wi}$ – longitudinal friction forces, $\mathbf{T}_{pi}$ – transverse friction forces, $\mathbf{N}_i$ – reaction deriving from the wheel load on the ground.

The forces occurring during motion in a single drive unit have been shown in Fig. 2. Gravity forces act on the mobile platform, reduced to the resultant value of the force $\mathbf{G}$ directed in the direction of the Z axis with the opposite sense, and the ground reaction represented by the forces $\mathbf{N}_i$ directed against the force of gravity. The platform remains at rest until the applied active forces reach the values exceeding the friction forces, which has been taken into account in the developed algorithm for numerical calculations of the system motion parameters. The drive torque has been selected in such a way as to meet the technical constraints resulting from the structure of the platform, which provides for the use of a brushless electric motor with a planetary gear [17].

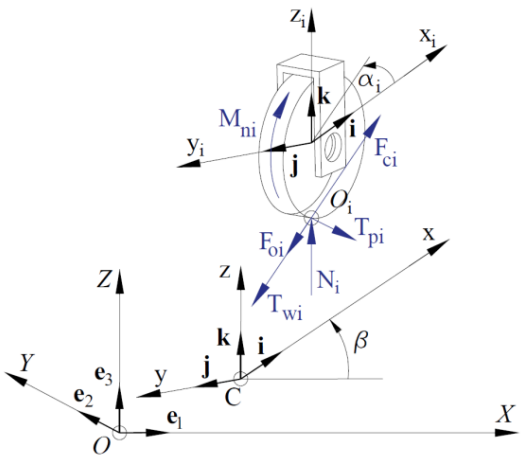

Fig. 2. Forces in the frame of reference during motion

The active forces have been determined from the dependence:

$$\mathbf{F}_{ci} = \begin{cases} \dfrac{\mathbf{M}_{ni}}{r_k} & \text{for} \quad \dfrac{\mathbf{M}_{ni}}{r_k} < \mathbf{T}_i, \\ \mathbf{T}_i & \text{for} \quad \dfrac{\mathbf{M}_{ni}}{r_k} \geq \mathbf{T}_i, \end{cases} \tag{4}$$

where: $\mathbf{M}_{ni}$ – drive torque, $\mathbf{T}_i$ – friction forces, r_k – wheel radius.

The friction forces begin to increase to the value of the developed friction forces from the moment when an active force is applied, which tends to induce a particular movement. The platform motion simulation results have been obtained taking into account the variable values of the active forces caused by the drive torque and changes in the position of the wheels during the platform motion, as well as the restistant forces opposing the active forces at the contact points of the wheels with the ground. If, during platform motion, values of friction forces have not been exceeded by the value of the quotient of the drive torque and the wheel radius, then the platform will move in a steady motion without skidding. However, if the value of the active force exceeds the value of developed friction, then wheel slip will occur. Forces of longitudinal and transverse friction have been determined from the relationship:

$$\begin{aligned} \mathbf{T}_{wi} &= -\mu_w \mathbf{N}_i \text{sign}(v_{wi})\mathbf{i}, \\ \mathbf{T}_{pi} &= -\mu_p \mathbf{N}_i \text{sign}(v_{pi})\mathbf{j}, \end{aligned} \tag{5}$$

where: μ_w and μ_p – friction coefficient in longitudinal and the transverse directions, v_{wi} and v_{pi} – linear velocities in longitudinal and the transverse directions.

Forces of resistance of motion $\mathbf{F}_{oi}$ represents forces deriving from the friction and from other factors occurring during platform motion, including air resistance, friction in motor bearings, etc.

Motion resistance forces have been determined as follows:

$$\mathbf{F}_{oi} = -f\,\mathbf{N}_i\,\text{sign}(v_{wi})\mathbf{i}, \tag{6}$$

where: f – motion resistance coefficient.

The solution to the problem of dynamics of motion of platform has been obtained using numerical calculation methods. The initial problem concerning the second-order ordinary differential equations has been solved using the Runge-Kutta fourth-order procedure. Finally, velocity vectors and a vector as a function of time have been determined, which made possible to determine the trajectory along which the platform moves and other parameters of the system motion. In the case of considering the motion of a plane platform, the previously formulated vector equations of motion can be replaced by equivalent systems of differential scalar equations, formulated in relation to the global coordinate system. If moments $\mathbf{M}_i$ from external forces have been omitted, scalar equations of motion of the center of mass C can be written. The equation of motion in the direction of the X and Y axes has been determined:

$$\ddot{X} = \frac{1}{m}\sum_{i=1}^{4} \mathrm{W}_{Xi}, \tag{7}$$

$$\ddot{Y} = \frac{1}{m}\sum_{i=1}^{4} \mathrm{W}_{Yi}, \tag{8}$$

where: m – total mass of the platform, W_{Xi} – resultant force on the X axis in the global reference frame, W_{Yi} – resultant force on the Y axis in the global reference frame.

The equation of motion around the center of mass C about the Z axis is given by the formula:

$$\ddot{\beta} = \frac{1}{\mathrm{I}_Z}\sum_{i=1}^{4} \mathrm{s}_{Xi}\mathrm{W}_{Yi} - \mathrm{s}_{Yi}\mathrm{W}_{Xi}, \tag{9}$$

where: I_Z – mass moment of inertia of the platform, W_{Xi} – resultant force on the X axis in the global reference frame, W_{Yi} – resultant force on the Y axis in the global reference frame, $\mathbf{s}_{Xi}$ – vector of position of resultant forces on the X axis of the global coordinate system, s_{Yi} – vector of position of resultant forces on the Y axis of the global coordinate system.

The model uses the ability to control the drive and position of each drive wheel during movement, and the dynamic interaction of the drive wheels with the ground is described. The algorithm includes the computational process by which the parameters of the mobile platform are determined. The platform is subjected to the force of gravity $\mathbf{G}$ and the ground reaction $\sum \mathbf{N}_i$ directed against the force of gravity. The difficulty in this procedure was to constantly track and determine, in each step of the integration, the current values of the active forces and friction forces, the relations of which affect the platform's behaviour. Tracking also requires establishing the relationship between the values of the active forces $\mathbf{F}_{ci}$ and the friction forces $\mathbf{T}_i$ at each time step. The active forces depend on the driving moments or their source is the kinetic energy accumulated in the system in the previous phase of the platform movement. On the basis of the adopted dynamics model and the initial data adopted in the work, a computational program in the Matlab environment has been built, using the proposed algorithm and own procedure for solving the initial problem using the Runge-Kutta method of the fourth order.

3. EXPERIMENTAL STUDIES WITH LEO ROVER

The results of experimental research, of which the main purpose was to verify and validate the adopted computational models for the dynamics of motion of wheeled mobile platforms [1], has been described in this part of the work. The results of the robots motion parameters have been gained on the basis of the input recording of the given configuration of the robot's wheel drive impulses and the recording of the real robot motion under the influence of these input forcings, while the motion recording covered a selected point of the robot body.

On the basis of these results, the effective values of the driving moments have been estimated, and the parameters of the robot's motion determined on the basis of the proposed computational model have been compared with the results read from the real robot's passage. Such a juxtaposition allowed to assess the compliance of the computer simulation results, determined with the use of a computational program based on the proposed in the paper motion dynamics model, with the results obtained from the recording of the real robot motion.

The experimental research has been carried out with the use of the LEO Rover robot (Fig. 3), which is designed to explore a variety of terrain.

The overall dimensions of the robot are as follows: length 414 mm × width 438 mm, and the robot with full accessories weighs 8 kg. A robot without full accessories (without a manipulator) has been used for the experimental tests, so the weight of the robot were 61 N.

The limitations resulting from the construction of the LEO Rover, i.e., low speeds or limitations of the camera range, resulting in achieving short travel routes and also achieving a linear velocity of up to 0.4 m/s while driving along a straight trajectory. The position of the robot's wheels is fixed in relation to the body, hence the turning of the robot is possible only by changing the velocity on individual wheels.

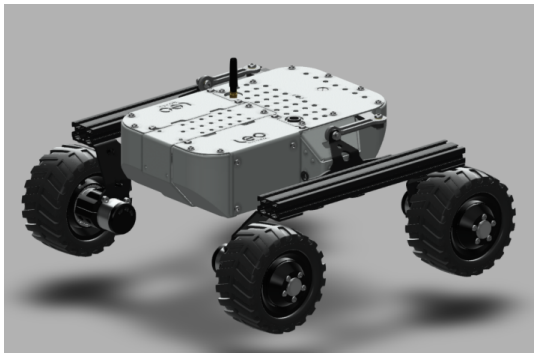

Fig. 3. LEO Rover model [18]

The test runs have been recorded and the test drives have been read using the *tracker* program (Fig. 4), where after the initial calibration of the robot's dimensions and the adoption of the tracking point, the motion parameters have been saved. The selected point of the robot body is the point indicated by the green arrow in Fig. 4.

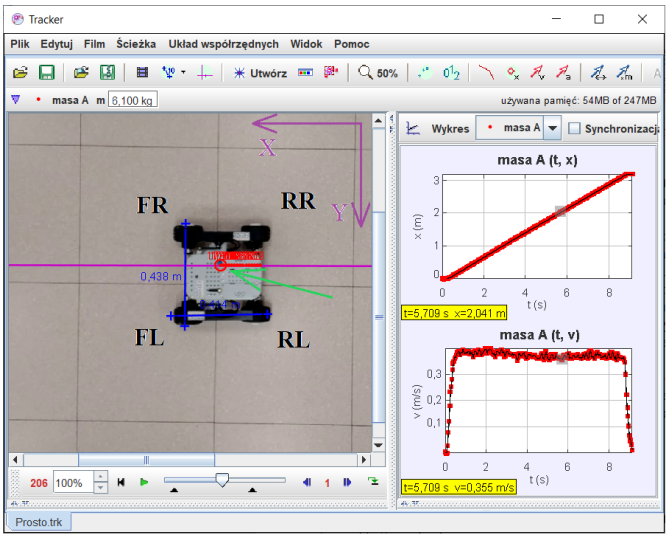

Fig. 4. A frame from a recording of a real robot's motion from the tracker software

The designations of the wheels, shown in Fig. 4, result from their position in relation to the direction of movement and the X axis, these are: FR – *front left*, FR – *front right*, RL – *rear left*, RR – *rear right*.

4. RESULTS OF EXPERIMENTAL RESEARCH

The tests consisted in registering the values of the forcings applied during subsequent attempts of the drive, each time the maximum values of the velocity, and then comparing them with

the values read from the recorded drive. In the next step, the obtained results have been compared with the motion simulation values. The values of the motion parameters for the rectilinear trajectory of motion have been obtained.

4.1. The results of the analysis of the forcings values with the real movement of the robot

The courses of the distances values have been determined on the basis of two data sets, i.e., one course based on the recording of the forced motion of the robot's wheels, and the other based on the recording of the real movement of the selected robot point, under the influence of the forcings imposed on the road wheels, have been shown in Fig. 5.

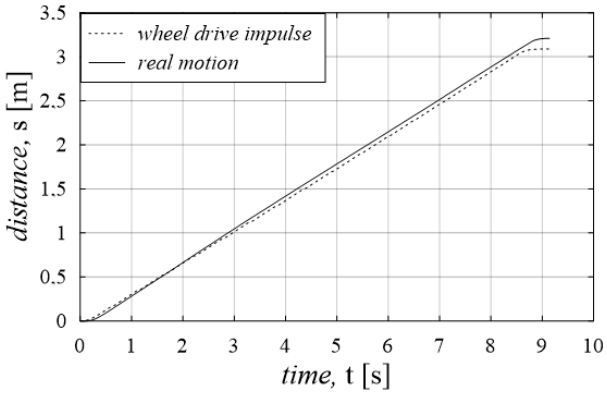

Fig. 5. The path of the LEO Rover robot in relation to the values of the set pulses of the wheel drives

In the first part of the movement, the recorded values of the displacement during the real robot's motion (determined on the basis of tracking the selected robot's point) are lower than those determined on the basis of the given wheel motion forces, which means that there is a slip between the wheel and the ground, because the wheels rotate faster than this is evidenced by the real trajectory of the robot.

In the last part of the movement, i.e., in the stage when the robot begins to brake, the behaviour changes, and the value of the distance travelled, recorded as the movement of the selected robot point, is higher than that determined on the basis of the record of the forces acting on the road wheels. This type of slippage is characteristic of vehicles in the braking phase, because as a result of stopping the wheels, they are no longer driven and the displacement progresses. Even at low velocity, the phenomenon of slippage can be observed.

On the basis of the obtained results, the course of the velocity has been compared (Figs. 6–8), paying particular attention to the places of velocity increase and decrease, i.e. the first and last phase of the movement, where the greatest discrepancies in the analysed values have been observed.

The velocities presented in Figs. 7, 8 represents the values obtained from the record of the angles of rotation of individual road wheels. The comparison of the velocity from the input of all drive wheels and the velocity from real motion of the observed robot point has been shown in Fig. 6.

The trajectory of the robot's motion along a rectilinear path has been shown in Fig. 9.

The next step of the research was to compare the results of the real robot's motion with the results of the motion simulation obtained on the basis of the proposed computational model of the robot's motion dynamics. The calculations have been made using the Matlab program.

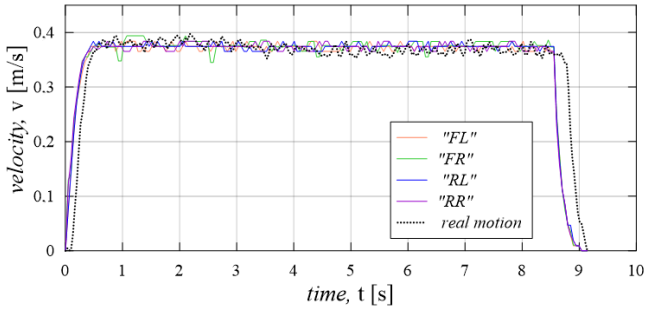

Fig. 6. The course of the velocity from the given impulses of the drive torques of the wheels during the entire movement with reference to the real motion

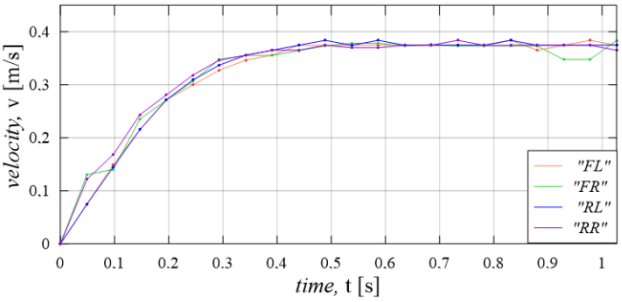

Fig. 7. The velocity course of the set pulses of the drive torques of the wheels in the first phase of the movement

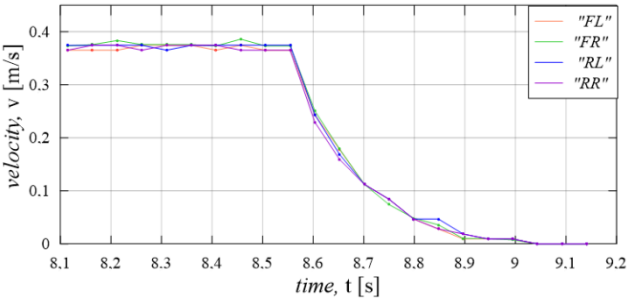

Fig. 8. The velocity course of the set pulses of the drive torques of the wheels in the last phase of the movement

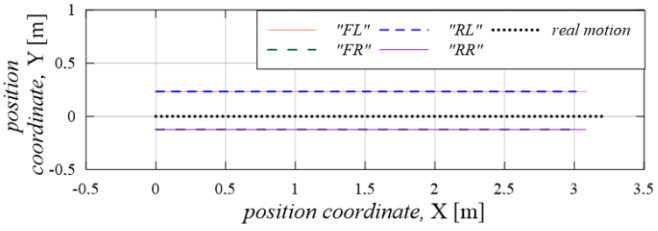

Fig. 9. Movement trajectory with the track of road wheels and a selected point of the robot's body in real motion

4.2. The results of the analysis of the real movement of the robot with simulation tests

The parameters listed in Table 1 have been adopted for the analysis.

Table 1
Initial values in experimental analysis

Initial conditions	Symbol	Value
Radius of the drive wheel [m]	r_k	0.064
Robot weight [N]	G	61
Effective drive torque [Nm]	M_{ne}	0.133
Friction coefficient in longitudinal direction	μ_w	0.7
Friction coefficient in transverse direction	μ_p	0.7
Initial position of robot's center of mass [m]	X, Y	[0; 0]
Total operating time [s]	t_c	9.141

The determined course of the effective drive torque, which has been adopted for the simulation tests, has been shown in Fig. 10. Effective drive torque should be understood as the excess of drive torque over the moment of resistance to motion.

The results of the velocity values determined experimentally and as a result of the numerical simulation have been shown in Fig. 11.

The comparison of the path determined experimentally and as a result of numerical simulation is shown in Fig. 12.

Based on the research, it has been shown that the relative difference in velocity in the time determined in the comparative analysis of the experimental method and numerical simulation in Matlab is $< 1\%$.

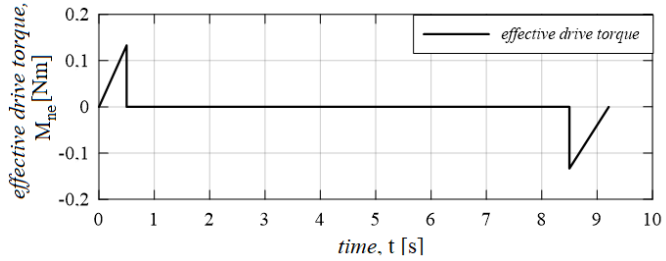

Fig. 10. Effective drive torque

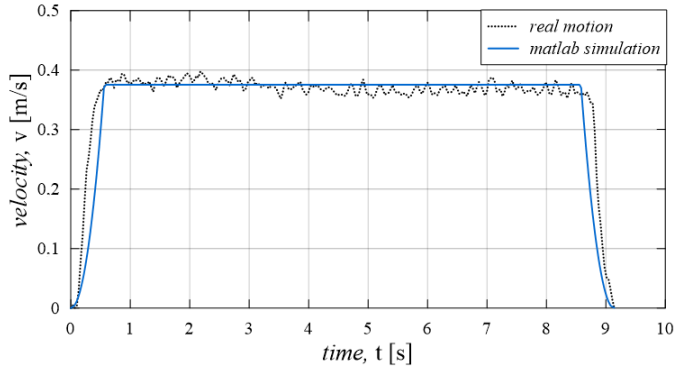

Fig. 11. Motion parameters in the form of velocities obtained as a result of experimental tests and numerical simulation

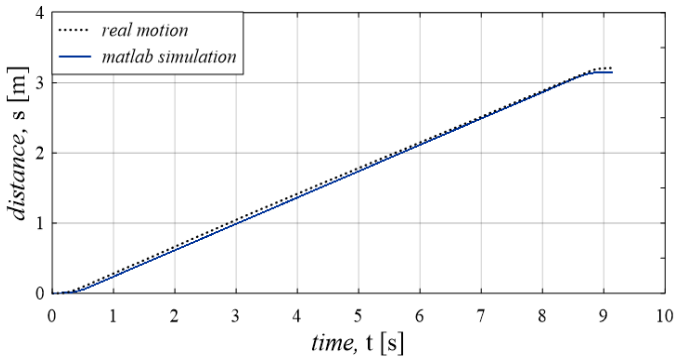

Fig. 12. Motion parameters in the form of a distance obtained as a result of experimental tests and numerical simulation

5. CONCLUSIONS

On the basis of the conducted experimental studies, the differences in the course of the displacements and the velocity obtained during the same runs have been indicated, which proves the existence of the phenomenon of slippage. The differences in the values of displacements, the courses of which have the same character along a rectilinear path, amount to 6.58%, and the velocity – less than 1%. On the basis of the initial data and the course of the robot's motion during the experimental tests, the parameters of the robot's motion in the form of robot displacements and velocities obtained on the basis of the computational model of the robot's dynamics as a result of computer simulation, have been determined. Compatibility has also been demonstrated for this method. As part of the verification of the robot's motion dynamics model, a comparison has been made of the nature and value of the waveforms of the motion parameters obtained by experimental means and simulation tests, showing the expected consistency of the results, both in the qualitative and quantitative sense. The proposed computational model can be useful in various situations, e.g., real-time control, where models with a high degree of complexity are useless due to the computation time. The simulation results obtained on the basis of the proposed model are sufficiently compatible with the results of experimental tests of motion parameters obtained for the selected type of mobile robot. The proposed dynamic model have been formulated in such a way that they can be modified and supplemented in order to carry out research on platform motion also in other conditions of non-flat ground, where during such tests it is necessary to consider the models of wheel-ground interaction, taking into account the ground topography.

REFERENCES

[1] A. Jaskot, "Modelowanie i analiza ruchu platform mobilnych z uwzględnieniem poślizgu," Ph.D. dissertation, Czestochowa University of Technology, 2021.

[2] Z. Lozia, "Modele symulacyjne ruchu i dynamiki dwóch pojazdów uprzywilejowanych," *Czaspismo Techniczne Mechanika*, vol. Z.8, pp. 19–34, 2012.

[3] S. Aguilera-Marinovic, M. Torres-Torriti, and F. Auat-Cheein, "General dynamic model for skid-steer mobile manipulators with wheel – ground interactions," *IEEE/ASME Transactions on Mechatronics*, vol. 22, no. 1, pp. 433–444, Feb. 2017, doi: 10.1109/tmech.2016.2601308.

[4] A. Mandow *et al*., "Experimental kinematics for wheeled skid-steer mobile robots," in *2007 IEEE/RSJ International Conference on Intelligent Robots and Systems*, IEEE, Oct. 2007, doi: 10.1109/iros.2007.4399139.

[5] D. Pazderski, "Waypoint following for differentially driven wheeled robots with limited velocity perturbations," *Journal of Intelligent & Robotic Systems*, vol. 85, no. 3–4, pp. 553–575, Jun. 2016, doi: 10.1007/s10846-016-0391-7.

[6] Y. Abdelgabar, J. Lee, and S. Okamoto, "Motion control of a three active wheeled mobile robot and collision-free human following navigation in outdoor environment," *Proc. Int. MultiConf. Eng. Comput. Sci*., vol. 1, p. 4, 2016.

[7] L. Xin, Q. Wang, J. She, and Y. Li, "Robust adaptive tracking control of wheeled mobile robot," *Rob. Auton. Syst*., vol. 78, pp. 36–48, 2016, doi: 10.1016/j.robot.2016.01.002.

[8] W. Kowalczyk and K. Kozłowski, "Trajectory tracking and collision avoidance for the formation of two-wheeled mobile robots," *Bull. Pol. Acad. Sci. Tech. Sci*., vol. 67, no. 5, pp. 915–924, 2019, doi: 10.24425/bpas.2019.128652.

[9] X. Feng and C.Wang, "Robust Adaptive Terminal Sliding Mode Control of an Omnidirectional Mobile Robot for Aircraft Skin Inspection," *Int. J. Control Autom. Syst*., vol. 19, no. 2, pp. 1078–1088, 2021, doi: 10.1007/s12555-020-0026-4.

[10] M. Nitulescu, "Solutions for Modeling and Control in Mobile Robotics," *J. Control Eng. Appl. Inf*., vol. 9, no. 3;4, pp. 43–50, 2007.

[11] D. Cekus, R. Gnatowska, and P. Kwiatoń, "Impact of Wind on the Movement of the Load Carried by Rotary Crane," *Appl. Sci*., vol. 9, no. 19, p. 22, 2019, doi: 10.3390/app9183842.

[12] A. Jaskot, B. Posiadała, and S. Śpiewak, "Dynamics Modelling of the Four-Wheeled Mobile Platform," *Mech. Res. Commun*., vol. 83, pp. 58–64, 2017, doi: 10.1016/j.mechrescom.2017.05.007.

[13] A. Jaskot, B. Posiadała, and S. Śpiewak, "Dynamics Model of the Mobile Platform for its Various Configurations," *Procedia Eng*., vol. 177, pp. 162–167, 2017, doi: 10.1016/j.proeng.2017.02.211.

[14] A. Jaskot and B. Posiadała, "Dynamics of the mobile platform with four wheel drive," *MATEC Web of Conferences*, vol. 254, p. 8, 2019, doi: 10.1051/matecconf/201925403006.

[15] N. Sarkar, X. Yun, and V. Kumar, "Control of Mechanical Systems With Rolling Constraints: Application to Dynamic Control of Mobile Robots," *Int. J. Rob. Res*., vol. 13, no. 1, pp. 55–69, 1994, doi: 10.1177/027836499401300104.

[16] M. Eghtesad and D. Necsulescu, "Study of the internal dynamics of an autonomous mobile robot," *Rob. Auton. Syst*., vol. 54, no. 4, pp. 342–349, 2006, doi: 10.1016/j.robot.2006.01.001.

[17] "Technical specification." [Online]. Available: http://pl.kwapil.com/downloads/maxon-ec-motor.pdf (Accessed 2017-07-24).

[18] "Leo rover specification." [Online]. Available: https://www.leorover.tech/the-rover (Accessed 2021-04-21).